Sterile inflammation in the spleen during atherosclerosis provides oxidation-specific epitopes that induce a protective B-cell response

Emilie K. Grasset[a], Amanda Duhlin[a,1], Hanna E. Agardh[b,1], Olga Ovchinnikova[b], Thomas Hägglöf[a], Mattias N. Forsell[a], Gabrielle Paulsson-Berne[b], Göran K. Hansson[b], Daniel F. J. Ketelhuth[b], and Mikael C. I. Karlsson[a,2]

[a]Department of Microbiology, Tumor and Cell Biology, Karolinska Institutet Solna Campus, Karolinska Institutet, SE-171 77 Stockholm, Sweden; and [b]Centre for Molecular Medicine, Karolinska Institutet, Karolinska University Hospital L8:01, SE-171 76 Stockholm, Sweden

The B-cell response in atherosclerosis is directed toward oxidation-specific epitopes such as phosphorylcholine (PC) that arise during disease-driven oxidation of self-antigens. PC-bearing antigens have been used to induce atheroprotective antibodies against modified low-density lipoproteins (oxLDL), leading to plaque reduction. Previous studies have found that B-cell transfer from aged atherosclerotic mice confers protection to young mice, but the mechanism is unknown. Here, we dissected the atheroprotective response in the spleen and found an ongoing germinal center reaction, accumulation of antibody-forming cells, and inflammasome activation in apolipoprotein E-deficient mice (Apoe$^{-/-}$). Specific B-cell clone expansion involved the heavy chain variable region (Vh) 5 and Vh7 B-cell receptor families that harbor anti-PC reactivity. oxLDL also accumulated in the spleen. To investigate whether protection could be induced by self-antigens alone, we injected apoptotic cells that carry the same oxidation-specific epitopes as oxLDL. This treatment reduced serum cholesterol and inhibited the development of atherosclerosis in a B-cell–dependent manner. Thus, we conclude that the spleen harbors a protective B-cell response that is initiated in atherosclerosis through sterile inflammation. These data highlight the importance of the spleen in atherosclerosis-associated immunity.

B cells | atherosclerosis | inflammasome

Our immune system has evolved to mediate protection against infections while maintaining homeostasis, including clearance of cellular debris and tissue repair. However, when unbalanced, the immune system is also involved in chronic inflammatory diseases such as atherosclerosis, and immune cells have long been known to be present in the atherosclerotic lesion (1, 2). The immune activation in lesions has therefore been intensively studied, and activated leukocytes such as T cells and macrophages found at this site have been determined to be involved in disease progression (3). The role of B cells in the plaque is less studied, but antibodies against oxidized low-density lipoprotein (oxLDL), as well as B cells, are found in plaques in both humans and mice (2, 4–9), and experimental studies show both atheroprotective and proatherosclerotic effects of B-cell populations (10–14).

Accumulation of cholesterol in the vessel wall leads to the generation of oxLDL, which drives vascular inflammation in a process that is thought to be important in the initiation of atherosclerosis (15). Modification of the accumulated lipids occurs through oxidative processes mediated in part by macrophages. The oxidation-specific epitopes that thereby arise from "modified self" can also be found on apoptotic cells, and antibodies against oxLDL are known to bind dying cells (16). An important sensor of modified self is the inflammasome, a cytoplasmic multiprotein complex that forms in response to inflammation. Of relevance for atherosclerosis, the NALP3 inflammasome can be activated by cholesterol crystals, resulting in activation of caspase-1, an enzyme that processes proinflammatory cytokines including IL-1 and IL-18 to their active forms (17–19). As this type of immune activation is not related to infection, it is referred to as sterile inflammation and is involved in the pathogenesis of a number of diseases (20).

Pattern recognition of oxidation-specific epitopes includes scavenger receptors cloned for their ability to bind oxLDL and germline-encoded antibodies produced by innate-type B cells. In this pool of antibodies, there are monospecific, as well as polyreactive, antibodies that bind multiple unrelated antigens. Among the monospecific inherited antibodies, one recombination event gives rise to an antibody recognizing phosphorylcholine (PC), named T15 (identical to the E06 antibody) (21, 22) This antibody, together with other antibodies to PC and modified LDL, has been associated with protection from atherosclerosis (23–28).

In mice and humans, the B1 cells (B1a and B1b) have been shown to be the main producers of natural antibodies at steady state and are found in the peritoneum, spleen, and bone marrow (29). The spleen is the major B2 B-cell reservoir, which harbors follicular B cells (FOB) and marginal zone B cells (MZB). MZB are innate-like cells that have been shown to be able to contribute to the anti-PC response to *Streptococcus pneumoniae* through a clone enriched in this population (M167), which binds to oxidation-specific epitopes in a similar manner to T15 (30, 31). In the marginal zone of the spleen, the MZB are in close contact with marginal zone macrophages (MZM) that express specific receptors, including the oxLDL-binding class A scavenger receptor macrophage receptor with collagenous structure (MARCO) (32).

In atherosclerosis, splenocyte transfer experiments from aged Apoe$^{-/-}$ to young splenectomized Apoe$^{-/-}$ mice show that the spleen confers an atheroprotective effect and that this is

Significance

In this study we investigate the origin of the protective B-cell response in the spleen in atherosclerosis. We find an ongoing B-cell activation with production of antibodies against oxidation-specific epitopes. In addition, this response can be accelerated using apoptotic cells alone that reduce lesion development and serum cholesterol in a B-cell–dependent manner. This study pinpoints the spleen as an important organ for atherosclerosis-associated immunity and provides novel pathways to use for treatment.

mediated by B cells (10). Experiments in which B-cell–deficient LDLr^{−/−} mice develop a more severe disease than B-cell–sufficient mice have further demonstrated a protective role for B cells (12). Removal of the spleen has been shown to deplete B1a cells from the peritoneum, and it was recently shown that transfer of these cells has an atheroprotective effect in splenectomized mice (11, 33), Thus, B1a cells have the ability to play an atheroprotective role in the absence of a spleen and as producers of natural T15 antibodies (11, 16, 26). However, MZB are also missing after splenectomy, and so far, dissection of B cells in the spleen of atherosclerotic Apoe^{−/−} mice has not been done.

We therefore set out to characterize the protective splenic B-cell response. Because cells of the marginal zone express an array of specific receptors for modified self-antigens, we hypothesized that an immune activation in this region could be the origin of the protective B-cell response in atherosclerosis. This would be in line with our previous data showing that apoptotic cells, carrying oxidation-specific epitopes (16), are trapped in the marginal zone (34). Because oxidation-specific epitope-bearing antigens give rise to antibodies binding oxLDL (25, 35), we also investigated the effects of immunization with apoptotic cells on atherosclerosis development, focusing on subpopulations of splenic B cells.

Our results show that hyperlipidemia associated with atherosclerosis by itself activates B cells in the spleen to produce large numbers of antibody-forming cells (AFC) secreting antibodies against oxidation-specific epitopes. We also find lipid accumulation and inflammasome activation in phagocytes that could drive this B-cell activation. Finally, we show that we can accelerate the protective response by administration of apoptotic cells, which results in reduced lesion size and cholesterol drop in serum.

Results

B-Cell Activation and Population Dynamics During Atherogenesis. To explore the effect that hyperlipidemia has on B cells in the spleen, young (6–8 wk) and old (21–22 wk) Apoe^{−/−} mice and age-matched wild-type C57BL/6 (WT) mice were investigated for B-cell precursors [transitional type 1 (T1) and type 2 (T2)] and naive B-cell populations (B1a, MZB, and FOB) (Fig. 1). The bone marrow-derived T1 precursors decreased with age in both strains, but to a significantly lesser extent in Apoe^{−/−} mice compared with in WT mice (Fig. 1A). The T2 stage, where selection into FOB and MZB pools takes place, also showed a decrease with age that was more pronounced in the Apoe^{−/−} strain (Fig. 1A). Contrasting the decrease in precursors, we found a significant increase of the MZB population with age in both strains. This increase was much more pronounced in old Apoe^{−/−} compared with WT mice, in line with previously published data (36). Only modest relative changes were seen in the FOB population in Apoe^{−/−} and WT mice, whereas the B1a compartment was decreased in the spleen of both WT and Apoe^{−/−} mice (Fig. 1B).

Investigating B1a and B1b cells in the peritoneal cavity, we found an increase in WT but no significant change in Apoe^{−/−} mice, showing that the reduction in B1 cells was not general (Fig. S1). The relative decrease seen in B-cell precursors is in line with previous data showing that decreased output from the bone marrow in older mice is accompanied by increased activation and proliferation in the peripheral B-cell compartment, in part compensating for the decreased output (37). Next we determined whether there was any evidence for B-cell activation other than the changes in naive populations. After activation, B cells can become IL-10–producing cells (B10) before differentiating further to AFC (38). As these cells have been shown to suppress inflammation in models of chronic inflammatory diseases, we investigated whether they accumulated in the spleen of Apoe^{−/−} mice. To our surprise, B cells were less prone to produce IL-10 in young as well as old Apoe^{−/−} mice compared with WT mice. The frequency of B10 cells significantly decreased with age, suggesting this population was not responsible for B-cell–dependent
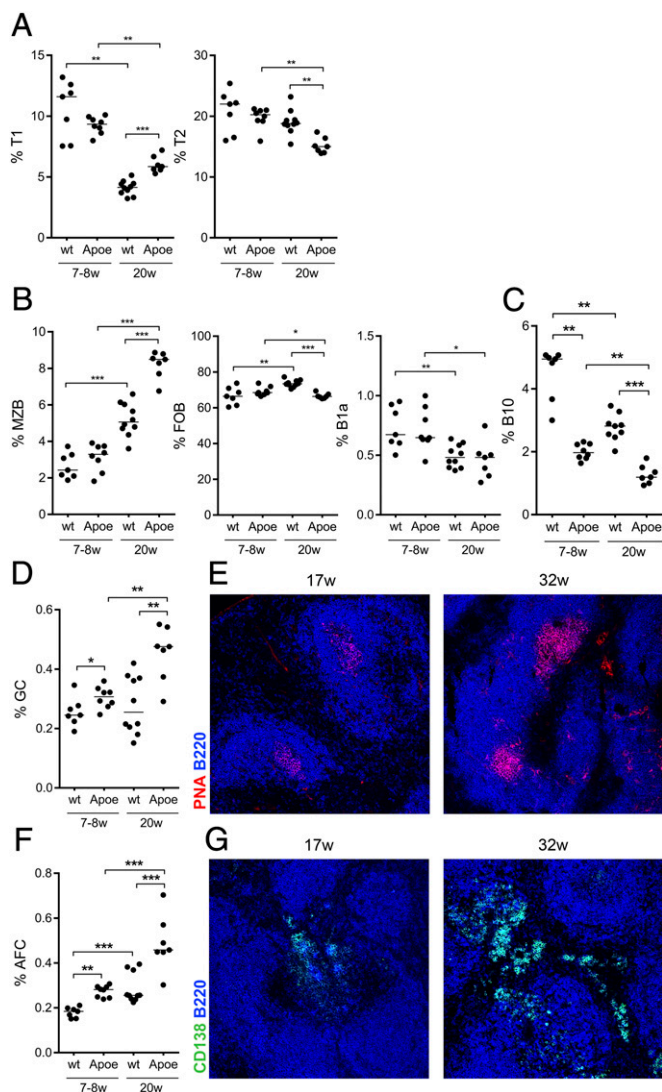

Fig. 1. Changes in naive B-cell populations and accumulation of germinal centers and antibody-forming cells in atherosclerotic Apoe^{−/−} mice. Transitional T1 T2 (A), naive (MZB, FOB, and splenic B1a cells) (B), and activated B-cell subpopulations; IL-10 producing B cells (B10) (C), GC (D), and AFC (F) were investigated in the spleens of young (7–8 wk) and old (20 wk) Apoe^{−/−} and C57BL/6 (WT) mice by flow cytometry. Median and individual mice (n = 7–10) are plotted. In addition, germinal center and antibody-secreting foci formation was imaged by immunofluorescence as PNA^{+}B220^{lo} (E) and CD138^{+}B220^{lo} (G), respectively. Data shown are representative of either one (C) or three (A, B, D, and F) experiments. Confocal images are representative of spleen images taken on sections from spleens of three (G, Left) to six (E and G, Right) mice. *P < 0.05, **P < 0.01, and ***P < 0.001 with a Mann–Whitney U test.

disease protection in previously published B-cell transfers (Fig. 1C).

There was a significant increase in germinal center B cells (GC) as well as AFC, implying an ongoing B-cell activation in aging mice. The GC and AFC populations were larger in old mice compared with younger mice in both strains, and there was a significant increase in Apoe^{−/−} mice compared with WT mice (Fig. 1 D and F). The GC and extrafollicular AFC foci were further confirmed by histology (Fig. 1 E and G). Thus, we found a striking expansion of the innate MZB subset as well as an ongoing adaptive B-cell activation in Apoe^{−/−} mice, with antibodies being produced by AFC residing in the red pulp of the spleen.

Selective Expansion and Activation of B-Cell Clones Reactive to PC and oxLDL. When mice and humans age, there is a reduced output of B cells from the bone marrow that is compensated for by peripheral expansion, driven in part by environmental antigens (37). Expanded B-cell populations in old $Apoe^{-/-}$ mice could therefore be a result of both age and disease, altering the selection and expansion of clones. To assess the clonal expansion of spleen B cells in aged $Apoe^{-/-}$ compared with WT mice, we performed spectratyping by amplifying the VDJ region of specific heavy chain variable region (Vh) families. In this assay, each peak represents clones with similar numbers of N-nucleotides. These clones are normally distributed in young, unimmunized WT mice. In both aged $Apoe^{-/-}$ and WT mice, we found changes in the B-cell pool with expansion of certain B-cell clones. This was true for the Vh1 family as well as for Vh3 and Vh9 (Fig. 2A and Fig. S2). However, in the Vh5 (7183) and Vh7 (S107) families, specific clones were expanded in $Apoe^{-/-}$ compared with WT mice (Fig. 2A). These

families are known to harbor the recombination combinations, giving rise to antibodies with anti-PC reactivity (22, 39, 40). To further investigate whether the response in old $Apoe^{-/-}$ mice was skewed toward anti-PC reactivity, we used an anti-T15 idiotype antibody to assess the frequency of T15$^+$ AFC in the spleen. A significantly larger number of AFC exhibited T15 reactivity in $Apoe^{-/-}$ compared with WT mice (Fig. 2B). Furthermore, this specificity was significantly increased with age in $Apoe^{-/-}$, but not in WT, mice (Fig. 2B). The anti-PC response was confirmed by ELISA, showing enhanced anti-PC IgM and IgG responses in young and old $Apoe^{-/-}$ mice compared with WT mice. In addition, anti-PC IgM levels increased with age in both strains (Fig. 2C). Because anti-PC antibodies recognize oxLDL, antibody levels were also measured using this antigen. A similar pattern was observed, with both young and old $Apoe^{-/-}$ mice displaying significantly higher IgM and IgG anti-oxLDL levels than WT mice (Fig. 2D). Whereas IgM anti-oxLDL increased with age in both strains, IgG antibodies to oxLDL increased with age only in $Apoe^{-/-}$ mice (Fig. 2D). In addition, we investigated the ability of the different subpopulations of B cells in the spleen to produce anti-PC antibodies by sorting MZB and FOB from $Apoe^{-/-}$ mice with subsequent stimulation in vitro (Fig. S3A). We found that MZB had a relatively higher anti-PC reactivity compared with FOB, using sorted peritoneal B1a cells as control. We then further addressed the question of the ability of MZB to confer the protection by transferring sorted MZB or FOB from old to young $Apoe^{-/-}$ mice. At 10 wk posttransfer, a trend could be seen in the MZB-transferred group toward an increase in anti-PC IgG antibodies (Fig. S3B). This could not be seen in the FOB-transferred group. Collectively, these data show that the response increased with age and disease development in $Apoe^{-/-}$ mice and skewed the aging B-cell pool, including enrichment for MZB harboring an inherited ability for anti-PC production.

Lipid Uptake in Spleen Cells Is Associated with Inflammasome Activation. Because we found evidence for anti-PC reactivity in spleens of aged $Apoe^{-/-}$ mice, we investigated the presence of lipid accumulation, which could provide antigen for a specific B-cell activation and drive the response. Interestingly, hyperlipidemia led to lipid accumulation in the spleen of $Apoe^{-/-}$ mice, with significant intracellular lipid accumulation in macrophages (Fig. 3A). Lipid accumulation has been shown to give rise to cholesterol crystals in macrophages (17), and using reflection microscopy, we also found evidence for occurrence of these crystals in the spleen (Fig. S4). Because intracellular oxLDL and/or cholesterol crystals can activate the inflammasome (17–19), we investigated the activity of the inflammasome component, caspase-1, in splenocytes by flow cytometry. Increased caspase-1 activation, detected as fluorescent labeled inhibitor of caspases (FLICA) positivity, was found in spleen monocytes (F4/80$^-$CD11b$^+$Ly6C$^+$), macrophages (F4/80$^+$CD11b$^+$), and neutrophils (Ly6G^{hi} CD11b^{hi}) of $Apoe^{-/-}$ compared with WT mice (Fig. 3B). The marginal zone is the interface between the spleen and the circulation, and its two major cell populations, MZM and MZB, both express scavenger receptors (41). We speculated that these cells may mediate lipid uptake in the spleen and tested this possibility after the accumulation of FITC-labeled oxLDL after i.v. injection. At 30 min postinjection, oxLDL was localized to the marginal zone of the spleen both within scavenger receptor MARCO$^+$ MZM (Fig. 3C) and through binding to MZB, as determined by flow cytometry (Fig. 3D). Although FOB showed some binding to oxLDL, we could not detect any oxLDL bound to B1a cells in the spleen. To investigate whether lipids taken up in the spleen were responsible for the observed inflammasome activation, we injected oxLDL and measured caspase-1 activity. We also investigated the effects of injecting syngeneic apoptotic cells that are known to target the marginal zone of the spleen (34). Either oxLDL or apoptotic cell
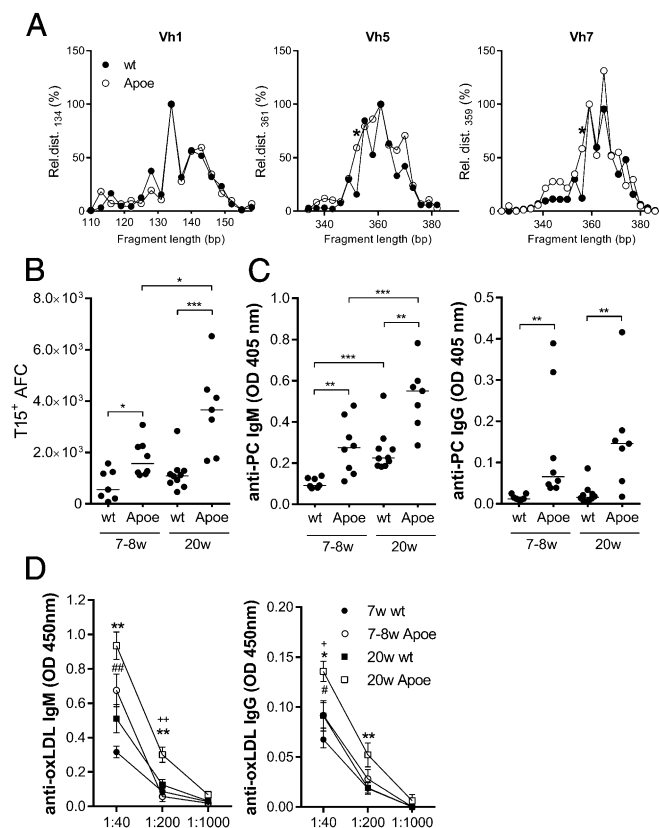

Fig. 2. Selective expansion and activation of B-cell clones reactive to PC and oxLDL. Clonal expansion was studied through spectratyping of splenocytes (A). The length (in nucleotides) of each detected fragment represents a clone, and the spectrum yielded of respective measured Vh family represents the clonal distribution. To account for experimental variation, we first normalized the area of each measured peak to an arbitrary peak of respective Vh family before comparing the relative clonal distribution (Rel.dist.) between the groups. Shown are Vh1 (*Left*), Vh5 (*Middle*), and Vh7 (*Right*). Each data point represents the median of eight individual mice. Because the Vh7 family harbors the T15 reactivity, we investigated the T15$^+$ AFC (CD138^{hi}B220^{lo}) in flow cytometry (B). Median and individual mice (n = 7–10) are plotted. Anti-PC (C) and anti-oxLDL (D) IgM (*Left*) and IgG (*Right*) levels were measured by ELISA in young and old $Apoe^{-/-}$ and WT mice. Median and individual mice (n = 7–10) are plotted (C). Mean and SEM from 7 to 10 mice are plotted (D). Data shown are representative of either one (A and B) or three (C and D) experiments. *P < 0.05, **P < 0.01, and ***P < 0.001 with a Mann–Whitney U test. In D, * is used to designate differences between old $Apoe^{-/-}$ and WT, # between young $Apoe^{-/-}$ and WT, and + between young and old $Apoe^{-/-}$ mice.
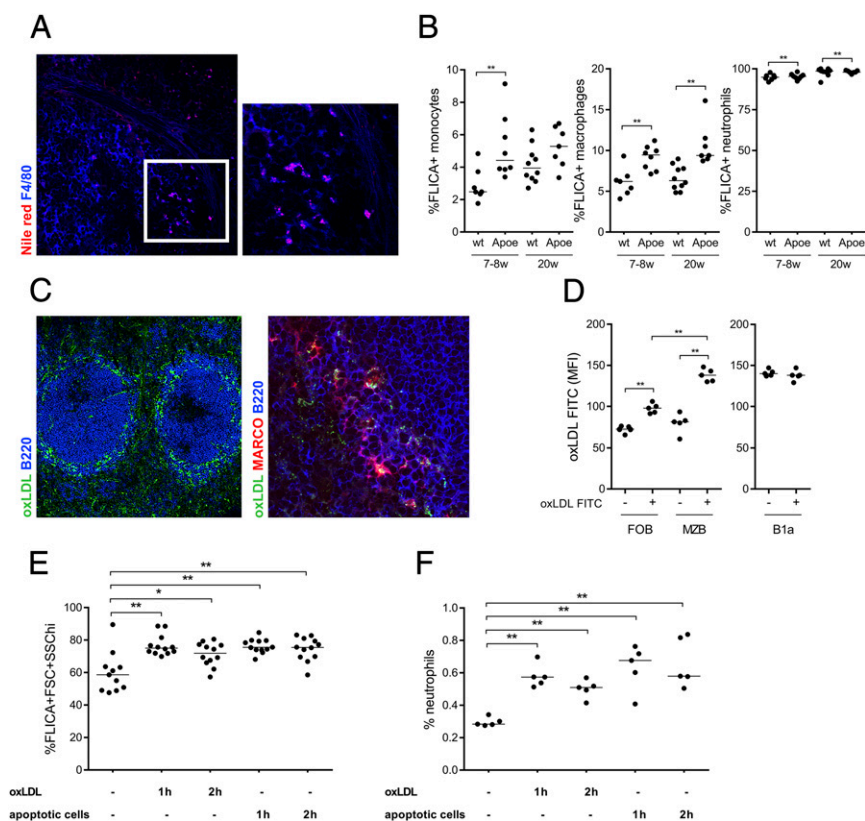
Fig. 3. Atherosclerosis induces lipid accumulation in the spleen, which drives inflammasome activation. Lipid accumulation in the spleen of old Apoe$^{-/-}$ was shown by Nile red lipid staining (red), and colocalization was seen with macrophages (F4/80$^+$, pseudo colored blue). Image was taken with 20× magnification (*Left*), and insert was magnified 2× (*A*). Inflammasome activation was studied through active caspase-1 (FLICA$^+$) in different cells' populations of the spleen by flow cytometry. FLICA$^+$ neutrophils (CD11b^{hi}Ly6G^{hi}) increased with age in both Apoe$^{-/-}$ and C57BL/6 (WT) mice (*B, Right*), whereas FLICA$^+$ macrophages (Ly6G$^-$F4/80$^+$CD11b$^+$) were increased in both young (7–8 wk) and old (20 w) Apoe$^{-/-}$ mice (*B, Middle*). Young Apoe$^{-/-}$ mice also have more FLICA$^+$CD11b$^+$Ly6C$^+$ monocytes compared with WT mice (*B, Left*). Median and individual mice (*n* = 7–10) are plotted. FITC-labeled oxLDL was injected i.v. to WT mice and shown by immunohistochemistry to localize to the marginal zone of the spleen after 30 min (*C, Left*), and more precisely to MARCO$^+$ MZM (*C, Right*). oxLDL-FITC binding to MZB (CD21^{hi}CD23^{lo}), FOB (CD23^{hi}CD21$^-$) (*D, Left*), and B1a (CD19^{hi}B220^{lo}CD5$^+$) (*D, Right*) was assessed by flow cytometry. Median and individual mice (*n* = 5) are plotted. One hundred micrograms oxLDL or 10^7 apoptotic cells were injected i.v., and inflammasome activation (*E*) and neutrophil recruitment (*F*) were studied in the spleen after 1 and 2 h by flow cytometry. Median and individual mice (*n* = 5–12) are plotted. Confocal images are representative of sections from spleens from five (*A*) and three (*C*) mice. Data shown are representative of either one (*B* and *F*) or three (*D*) experiments or pooled data from three experiments (*E*). *n* = 3–10 in each experiment. *P < 0.05 and **P < 0.01 with a Mann–Whitney *U* test.

injections lead to caspase-1 activation (Fig. 3*E*). In addition, both antigens separately recruited neutrophils to the spleen, a sign of local inflammation (Fig. 3*F*). Thus, lipids accumulating in the spleen of old Apoe$^{-/-}$ mice can promote inflammasome activation, explaining the ongoing B-cell response. In addition, either oxLDL or apoptotic cells carrying oxidation-specific epitopes can be recognized and taken up in the marginal zone of the spleen and result in inflammasome activation.

Apoptotic Cell Injections Protect Against Lesion Development and Lower Cholesterol in a B-Cell–Dependent Manner. It has previously been shown that injection of foreign antigens carrying oxidation-specific epitopes gives rise to an anti-PC response that reduces atherosclerosis (25). Here, we wanted to test whether the inflammasome-driven sterile inflammation in the marginal zone of the spleen could enhance a B-cell response toward oxidation-specific epitopes similar to that seen in atherosclerotic Apoe$^{-/-}$ mice. Syngeneic apoptotic cells were injected in WT and Apoe$^{-/-}$ mice six times during disease development i.v. in an attempt to enhance the B-cell response in the spleen (Fig. 4*A*). Blood samples were taken throughout the experiment, and at 17 weeks of age, the mice were evaluated for disease development. This treatment had a profound positive disease-preventing effect in Apoe$^{-/-}$ mice and resulted in

significantly reduced lesions compared with control Apoe$^{-/-}$ mice, both in the aortic root (Fig. 4 *B* and *C*) and in en face preparations of the thoracic aorta (Fig. 4*D*). Apoptotic cell injections also significantly lowered cholesterol levels both in Apoe$^{-/-}$ and WT mice (Fig. 4*E*). To investigate whether this effect was B-cell–dependent, we injected apoptotic cells into B-cell–deficient µMTApoe$^{-/-}$ mice. The drop in cholesterol could not be seen in µMTApoe$^{-/-}$ mice, implying that this effect of apoptotic cells was B-cell–dependent. In addition, cholesterol levels were higher in B-cell–deficient Apoe$^{-/-}$ mice after four injections of apoptotic cells (Fig. 4*E*). Analysis of atherosclerotic lesions in en face preparations of the thoracic aorta of µMTApoe$^{-/-}$ mice did not show any change after injection of apoptotic cells, implying that B cells were required to elicit an atheroprotective effect induced by these PC-containing antigens (Fig. 4*F*).

The Atheroprotective B-Cell Response Induced by Apoptotic Cells Is Similar to That Seen in Aged Apoe$^{-/-}$ Mice. We next investigated B-cell populations and activation in mice injected with apoptotic cells. The MZB cell population was increased in Apoe$^{-/-}$ compared with WT mice, but was not affected by apoptotic cell injections (Fig. 5*A*). In addition, apoptotic cells showed no effect on the peritoneal B1 populations ([Fig. S5](#)). In contrast, germinal
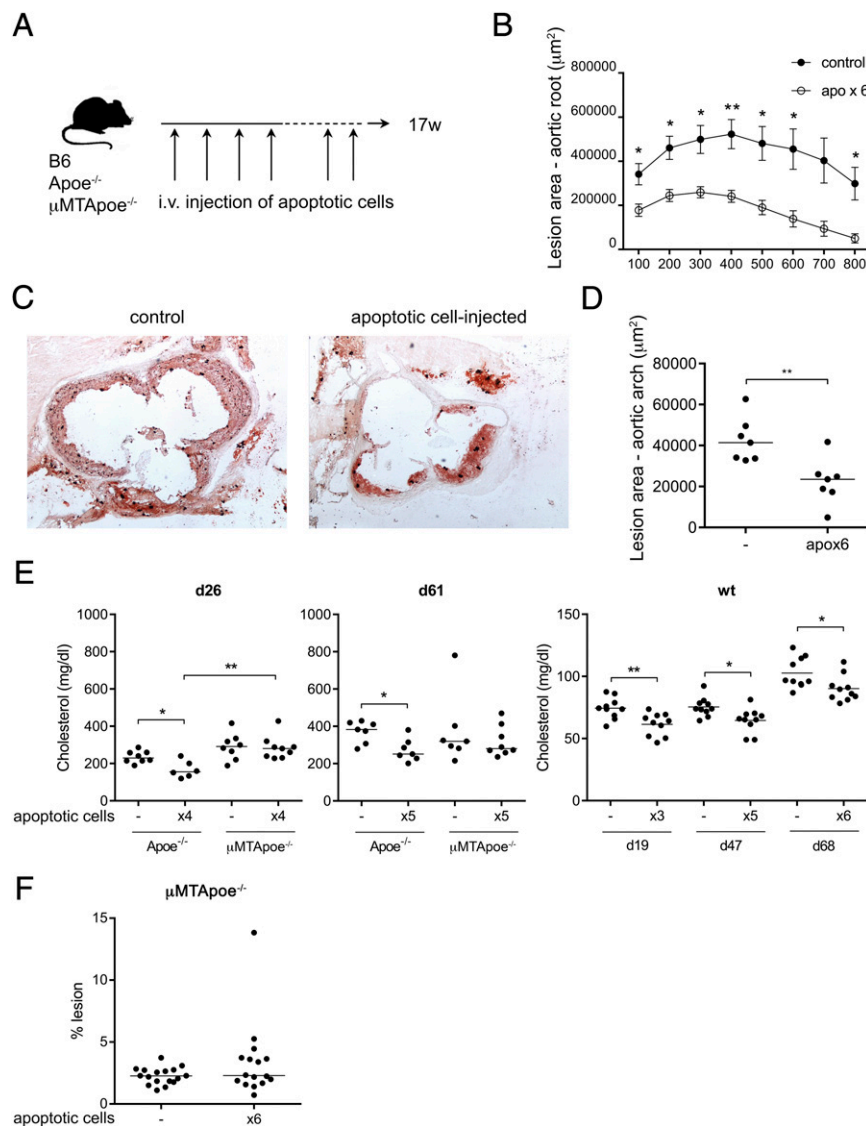
Fig. 4. Apoptotic cell injections protect against lesion development and lower cholesterol in a B-cell-dependent way. Apoe$^{-/-}$ and C57BL/6 (WT) mice were injected six times with apoptotic cells during disease progression, as indicated by the scheme shown in A. Aortic lesions in the aortic root, assessed by oil red O staining, showed reduced lesions in apoptotic cell-injected Apoe$^{-/-}$ compared with uninjected controls (C), quantified as lesion area (B). Lesion in aortas assessed by Sudan IV staining in D and F. Median and individual mice [$n = 6–7$ (D); $n = 16–17$ (F)] are plotted. Cholesterol levels, measured using enzymatic colorimetric assays, in apoptotic cell-injected (×3, ×4, ×5, or ×6) Apoe$^{-/-}$, µMTApoe$^{-/-}$, or WT mice compared with uninjected (−) age-matched controls at indicated days after the first injection (E). Median (*Left* and *Middle*) or mean (*Right*) and individual mice ($n = 6–10$) are plotted. Data shown from one experiment in which $n = 5–8$ (B and C), a separate experiment in which $n = 7$ (D), representative of 2 experiments in which $n = 6–10$ (E), pooled from two and representative of three experiments in which $n = 3–9$ (µMTApoe$^{-/-}$ in E) or pooled from three experiments (F). *$P < 0.05$ and **$P < 0.01$ by a Mann–Whitney U test or Student's *t* test in E (*Right*).

centers as well as AFC were increased in both groups of mice after apoptotic cell injections (Fig. 5B). Apoe$^{-/-}$ mice had more GC B cells and AFC compared with WT mice, both before and after treatment. When investigating AFC specificity, we found an increase in the proportion of T15$^+$ AFC after apoptotic cell injections (Fig. 5C) concomitant with increased titers of anti-oxLDL antibodies (Fig. 5D). To further investigate whether the antibody response to apoptotic cells was dependent on inflammasome activation, we injected NOD-like receptor family, pyrin domain containing 3 (nlrp3)-deficient mice four times with apoptotic cells and studied the anti-PC response. In naive mice, the percentage of MZB was reduced in the spleen of nlrp3$^{-/-}$, whereas no difference was seen in the FOB or B1a compartment (Fig. S6A). After injections of apoptotic cells, both the anti-PC IgM and IgG response was NALP3-dependent, as no significant

induction was seen in nlrp3-deficient mice (Fig. S6B). To further link caspase-1 activation to this B-cell phenotype, we injected the inflammasome-derived cytokine IL-18 into CD19-deficient mice that lack MZB and B1 cells. In line with the data in the nlrp3$^{-/-}$, IL-18 injections gave rise to MZB and B1a expansion in the spleen (Fig. S6C), whereas no expansion of FOB or peritoneal B1a was seen.

Thus, administration of apoptotic cells gives rise to an oxidation-specific antibody response in the spleen, including anti-PC, and this response lowers cholesterol levels and inhibits atherosclerosis development. Together, these data show that a splenic sterile inflammatory response gives rise to activation of a protective B-cell response in the spleen that has beneficial effects on lipid levels as well as lesion development. They also pinpoint the
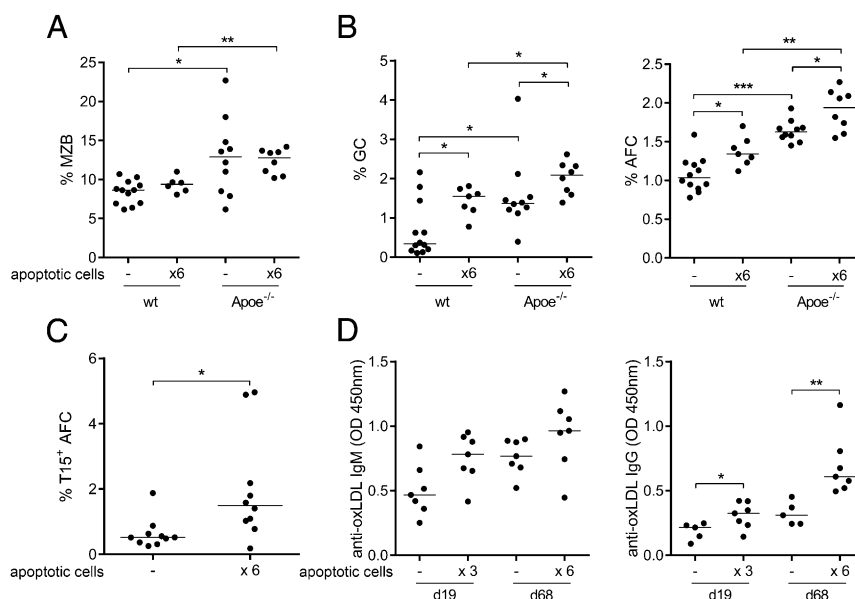
Fig. 5. The atheroprotective B-cell response induced by apoptotic cells is similar to that seen in aged Apoe$^{-/-}$ mice. Spleens of noninjected (−) and apoptotic cell-injected (×6) Apoe$^{-/-}$ and C57BL/6 (WT) mice were investigated for MZB (*A*) and activated B cells (*B*); GC B cells (*Left*), and AFC (*Right*) by flow cytometry. In WT mice, T15 idiotype-positive AFC were assessed (*C*), and anti-oxLDL IgM and IgG was measured by ELISA (*D*). Median and individual mice (*n* = 5–12) are plotted (*A*–*D*). Mean and individual mice (*n* = 14–18) are plotted. Data shown from one representative of two experiments, *n* = 10 (*C*), representative of two, *n* = 5–12 (*A*, *B*, and *D*). *$P < 0.05$, **$P < 0.01$, and ***$P < 0.001$ by a Mann–Whitney *U* test.

spleen as an important organ for studies on immune activation in atherosclerosis.

Discussion

Several studies point to an important atheroprotective role of humoral immunity. We now show that an immune response develops in the spleen of hypercholesterolemic Apoe$^{-/-}$ mice, with uptake of oxLDL in the marginal zone and increased numbers of GC B cells and AFC. This response involves clonal expansion of the Vh5 and Vh7 BCR families known to harbor anti-PC reactivity. Intravenous injections of apoptotic cells carrying oxidized surface PC attenuates hypercholesterolemia and reduces atherosclerosis in a B-cell–dependent process. These data show that atheroprotective immunity is elicited by oxidation-specific epitopes generated in hypercholesterolemia and identify spleen B cells as important mediators of this response.

We hypothesized that the increased and skewed B-cell activation in Apoe$^{-/-}$ mice could be a result of chronic stimulation and selection driven by lipid accumulation in the spleen. This would be in line with previous data showing lipid accumulation in the spleens of LDLr$^{-/-}$ transferred with ABCA1/ABCG1 double-deficient bone marrow (42). Indeed, we found evidence for lipid accumulation in the spleen of Apoe$^{-/-}$ mice, where it could be driving sterile inflammation. A sensor of sterile inflammation, the NALP3 inflammasome, has been shown to be activated by cholesterol crystals leading to caspase-1 (17). We found evidence for activation of this pathway with increased caspase-1 activation in Apoe$^{-/-}$ mice compared with WT, indicating that increased inflammasome activation was connected to disease progression. Systemic administration of oxLDL and apoptotic cells leads to caspase-1 activation in the spleen, and apoptotic cells failed to induce an anti-PC antibody response in the absence of NALP3. Together, these data suggested that lipid accumulation including crystal formation provided activatory signals as well as antigen that skewed the B-cell pool and selection of clones in Apoe$^{-/-}$ mice. We further showed that apoptotic cell injections induced a B-cell–dependent reduction of atherosclerotic lesions and systemic cholesterol levels. This protective response coincided with

an increase in anti-oxLDL antibodies. Vaccination strategies using *S. pneumoniae*, MDA-LDL, and PC, all giving rise to an anti-PC response, as well as passive immunization using anti-PC antibodies, have all been shown to reduce plaque formation. We show here that self-antigens in the absence of adjuvant also could provide this protection. The beneficial effect of IgM antibodies is believed to be a result of several effector functions (reviewed in ref. 43). These include blocking uptake of oxLDL, inhibition of foam cell activation, sequestering of oxLDL from the plaque, and finally, aiding in clearing apoptotic cells in the plaque itself.

The lesion decrease in Apoe$^{-/-}$ mice injected with apoptotic cells was further accompanied by the same phenotype of spleen B-cell subpopulations as seen in aging Apoe$^{-/-}$ mice, suggesting that the protection was mediated through spleen B cells. The question remains: Which B-cell populations in the spleen are recruited to the AFC pool? It has been convincingly shown that B1a cells have the ability to produce natural IgM that can protect from atherosclerosis (26). In particular, B1a cells are the main producers of the anti-PC T15 idiotype (44). In the recent publication by Kyaw et al., transfer of B1a cells from peritoneal cavity has a protective effect on plaque development in splenectomized mice lacking this subset (11). We found that peritoneal B1 expanded with age in WT and Apoe$^{-/-}$ mice, which might also support a role for B1a in this model. However, even though splenectomy decreases B1a cells in the peritoneum, it also removes the marginal zone that is the niche needed for development of MZB (33). In addition, B1a cells are generally rare in the spleen, and we did not see an increased proportion of B1a cells with age in Apoe$^{-/-}$ mice, nor following the injection of apoptotic cells. Therefore, the protective effect carried by peritoneal B1a cells or by spleen B1a cells after immunization does not explain the protective effect seen when transferring total spleen B cells (10).

Other subpopulations of B cells could be contributing to the lipid accumulation-driven protective response seen in old Apoe$^{-/-}$ mice. Of interest, *S. pneumoniae* administered i.v. recruits not only B1a but also MZB to the early burst in IgM-producing plasma cells (31). This is in contrast with low-dose i.p. immunization, in which the response is almost exclusively derived from B1a cells.

Because oxLDL is found in the circulation of hypercholesterolemic mice, and we here found that MZB are expanded in Apoe$^{-/-}$ mice and directly bound to oxLDL, these cells could be activated to produce plasmablasts toward modified self. In addition, it has been shown that the MZB contribution to the anti-PC response to *S. pneumoniae* is proportional to the frequency of anti-PC clones present in the preimmune repertoire (31).

Although B1a and MZB have previously been compared in WT mice for their capacity to produce anti-PC antibodies (26), this had not been done in Apoe$^{-/-}$ mice. Our data showed that all three subtypes could produce anti-PC IgM, with the most efficient producer being peritoneal B1a cells, followed by MZB and, to a lesser extent, FOB. We further addressed the ability of precursors to give rise to the response by transferring sorted MZB and FOB from old to young Apoe$^{-/-}$ mice. In the MZB-transferred group, a trend toward an increase in anti-PC IgG could be seen, whereas no increase was seen in the FOB-transferred group. Because injections of the inflammasome-derived cytokine IL-18 also gave rise to MZB and splenic B1a, but not peritoneal B1 cells, it is likely that sterile inflammation leads to an activation of splenic innate B cells, which in turn leads to a protective anti-PC response. Even though our data point toward involvement of MZB in the protective response, we cannot exclude contribution of, especially, B1a cells in the spleen and believe that the response is likely a collaborative B-cell effort.

Lately, the view that B cells have a protective role in atherosclerosis has been challenged somewhat by B2 B-cell transfers to lymphocyte-deficient Apoe$^{-/-}$ mice showing worsening of disease, as well as by the atheroprotective effect mediated by anti-CD20 B-cell depletion (13, 14). These, at first glance contradictory, results from anti-CD20 depletion of B cells might shed some light on different roles for different B-cell populations in atherosclerosis. Anti-CD20 depletion leads to a pronounced reduction in IgG anti-oxLDL antibodies, as well as a reduction of T-cell activation. However, IgM anti-oxLDL levels are less reduced, which is consistent with the fact that peritoneal B1a cells are less efficiently depleted by anti-CD20 therapy (45). There is also some evidence that MZB might not be as efficiently depleted by anti-CD20 therapy (46). These data suggest that FOB, which more readily switch to IgG and participate in T-cell–dependent responses, might be proatherogenic, whereas the atheroprotective effect lies within the B1a cell and possibly MZB populations.

In conclusion, we found that the protective effect seen in transfer experiments from old Apoe$^{-/-}$ mice was a result of the transfer of a large number of plasma cells producing antibodies toward oxidation-specific epitopes. In addition, systemic administration of apoptotic cells carrying oxidation-specific epitopes induced the atheroprotective response in the spleen. The drop in lesion size was paralleled by a decrease of serum cholesterol levels, and both effects were shown to be B-cell–dependent. These findings pinpoint the spleen as an important source of immune activation in atherosclerosis and are in line with what has been described in previous publications linking splenectomy in humans with cholesterol and/or heart disease (47, 48). We believe that the link between the spleen and cardiovascular disease will be important for future research in connection to the activation of T cells known to be important for atherosclerosis development.

Materials and Methods

Experimental Animals. Apoe$^{-/-}$ mice were obtained from the animal facility of the Centre for Molecular Medicine or Taconic, C57BL/6 mice were obtained from Charles River or from the animal facility of the Department of Microbiology, Tumor and Cell Biology, and B-cell–deficient μMTApoe$^{-/-}$ mice were obtained from the Centre for Molecular Medicine. Animals were kept and bred under specific pathogen-free conditions at the animal facilities of the Department of Microbiology, Tumor and Cell Biology and the Centre for Molecular Medicine. All experiments were approved by the local ethical committee (North Stockholm district court).

Lipoprotein Preparations. LDL (d = 1.019–1.063 g/mL) was isolated by ultracentrifugation from pooled plasma of healthy donors, as described (49), and 2 mM benzamidine, 0.5 mM PMSF, and 0.1 U/mL aprotinin were added immediately after the plasma was prepared. After isolation, LDL was dialyzed extensively against PBS. One millimole EDTA was added to an aliquot of LDL to generate unmodified LDL. Oxidized LDL was obtained by incubating 1 mL LDL (1 mg/mL protein content, determined by Bradford assay; Biorad) in the presence of 20 μM CuSO$_4$ for 18 h at 37 °C. The extent of oxidation was evaluated by thiobarbituric acid-reactive substances (TBARS), as described (50).

Preparation of FITC-Labeled LDL. LDL was labeled as previously described (51). Briefly, LDL (1.5–2 mg/mL) was dialyzed overnight against 500 mmol/L NaHCO$_3$ at pH 9.5. Next, 100 μg FITC (Sigma-Aldrich) dissolved in DMSO (1 mg/mL) was added for each milligram of LDL and incubated at room temperature for 2 h. After incubation, conjugates were separated from the free fluorochrome by filtration on a PD 10 column (GE Healthcare Life Sciences) using PBS for elution. FITC concentration in LDL preparations was measured by absorption spectroscopy against FITC standard at 495 nm. Protein concentration was determined by Bradford assay (BioRad).

Immunizations and Cell Culture. Apoptosis in thymocytes was induced by dexamethasone treatment for 6 h, after which cells were washed twice in PBS. Mice were immunized i.v. with 10^7 syngeneic apoptotic thymocytes without adjuvant first 4 times weekly and then every third week to maintain autoantibody titers (52). One hundred micrograms FITC-labeled oxLDL was injected once, and localization of oxLDL was assessed after 30 min. B10 and B10 precursors were assessed as previously described (53). Briefly, splenocytes were put in culture and stimulated with LPS for 48 h. During the last 5 h, PMA ionomycin and brefeldin A were added to the cultures. Unstimulated cells where only brefeldin A was added the last 5 h were used as controls. After stimulation, IL-10 producing B cells were investigated by flow cytometry.

Flow Cytometry. Splenocytes or peritoneal exudate in single-cell suspension were first blocked with purified anti-mouse CD16/32 (BD) to reduce unspecific binding and were stained with the LIVE/DEAD fixable stain kit (Invitrogen) to exclude dead cells. The cells were then stained with antibodies against mouse B220, CD1d, CD5, CD11c, CD11b, CD19, CD21, CD23, CD38, CD95, CD138, F4/80, GL7, IAb, IgM, Ly6C, Ly6G, TCRβ (BD, Biolegend), and fluorescently labeled streptavidin (BD, Biolegend). For intracellular staining of IgD, IgM, IgE, IgG1, IgG2, and IgG3, cells were fixed and permeabilized using Biolegend buffers according to manufacturer's instructions. The different subpopulations of B cells were defined according to Table S1. Anti-T15 idiotype antibody was kindly provided by Chris Heusser (Novartis), and alexa647-conjugated according to manufacturer's instructions (Invitrogen). The active caspase-1–binding fluorescent probe FLICA was used according to manufacturer's instructions (ImmunoChemistry Technologies). Samples were analyzed on a FACSCalibur, FACSAria, or FACSFortessa (Becton Dickinson), using FlowJo software.

Histology. Spleens were frozen in OCT (Bio-Optica), cut to 8-μm sections in a cryostat microtome, fixed in acetone, blocked with biotin/avidin blocking kit (Vector Laboratories) and goat serum (Dako), and stained with anti-mouse B220 (RA3-6B2) (Biolegend), MARCO (ED31), and CD138 (281-2) antibodies (BD) and peanut agglutinin (PNA) (Vector Laboratories). For lipid staining, sections were blocked with goat serum and stained with the lipid dye Nile red (Sigma-Aldrich), together with an anti-F4/80 antibody (BM8) (Biolegend). Images were collected using a confocal laser scanning microscope (Leica TCS SP2, DMIRBE) equipped with one argon and two HeNe lasers and processed in Photoshop software (Adobe Systems).

ELISA. Serum antibodies were measured using standard ELISA techniques. Specific IgG and IgM antibodies against PC and oxLDL were captured with PC-BSA and oxLDL, as described previously. Anti-PC antibodies were detected with AP-conjugated secondary anti-mouse IgM and IgG, whereas anti-oxLDL antibodies were detected with biotinylated anti-mouse IgM and IgG, followed by streptavidin-HRP.

Lipid Measurement. Serum triglycerides and cholesterol levels were measured using enzymatic colorimetric kits (Randox Laboratory, Ltd.) according to the manufacturer's protocol.

Spectratyping. The B-cell repertoire of WT and Apoe$^{-/-}$ mice was assessed by spectratyping of VDJ regions of heavy chain families 1, 3, 5, 7, and 9 (Vh1,

Vh3, Vh5, Vh7, and Vh9, respectively). Briefly, mRNA from 5×10^5 or 1×10^6 freshly isolated splenocytes was extracted with an RNAeasy kit (Invitrogen), and cDNA was subsequently generated from 2 μL mRNA, using iScript (BioRad), according to the manufacturer's instructions. Previously published primers for amplification of the VDJ-region of Vh1, Vh3, Vh5, and Vh7 were used to amplify the target regions [Vh1 forward: TCCAGCACAGCCTACA-TGCAGCTC; Vh3 forward: AGGTGCAGCTTCAGGAGTCAGG; Vh5 forward: C-AGCTGGTGGAGTCTGGGGGA; Vh7 forward: AGGTGAAGCTGGTGGAGTCTGG; Jrev (common primer in the JH-region): CTTACCTGAGGAGACGGTGA] (54). The forward primer for Vh9 was designed in-house to anneal to published Vh9 sequences (forward: CAGTTGGTGCAGTCTGGACCT). The amplifications were performed in a total volume of 20 μL, using 2× GoTaq (Promega), 2 μL (1 μM final) of each primer, and 2 μL of cDNA. After 1 min at 95 °C, amplification was performed for 40 cycles as follows: 30 s at 95 °C, 30 s at 55 °C, and 1 min 30 s at 72 °C, and ended with a step of 10 min at 72 °C. To label the amplified fragments, 5 μL of each PCR product was mixed with 0.5 μM 6-fluorescein amidite (FAM)-labeled Jrev-primer and 5 μL GoTaq and subjected to 10 runoff cycles as follows: 2 min at 95 °C, 2 min at 55 °C, and 20 min at 72 °C, and ended with a 10-min step at 72 °C. FAM-labeled products were then processed on an ABI3130 Genetic analyzer (Applied Biosystems). Spectratype data were analyzed using PeakScanner v1.0 software (Applied Biosystems), where the length (in nucleotides) of each detected fragment represents a clone and the spectrum yielded of respective measured Vh-family represents the clonal distribution. To account for experimental variation, we first normalized the area of each measured peak to an arbitrary peak of respective Vh family before comparing the relative clonal distribution between the groups.

Lesion Measurement. Hearts and aortas were collected from perfused mice. Hearts were serially sectioned from the proximal 1 mm of the aortic root on a cryostat. Oil red O- and hematoxylin-stained sections were used to evaluate lesion size. Lesion size was determined by measuring eight oil red O- and hematoxylin-stained sections, collected at every 100 μm over a 1-mm segment of the aortic root (55). Aortas were collected from mice using microdissection and kept in 4% (wt/vol) paraformaldehyde for at least 24 h until pinning. Aortas were cut open from the arch, including the branches, all of the way down through the thoracic part, and pinned on a bed of Parafilm, using Austerlitz insect pins minutien d0.10 mm. Pinned aortas were stored in PBS until staining and then rinsed in 70% (vol/vol) ethanol for 5 min, stained in Sudan IV staining solution [5 g Sudan IV (Merch Eurolab), 500 mL 70% (vol/vol) ethanol, 500 mL 100% acetone] for 6–8 min, rinsed in 80% (vol/vol) ethanol twice for 3 min, and last, rinsed in PBS. A Leica camera DC480 on a Leica MZ6 microscope was used for acquiring images of the stained aortas, and ImageJ was used for analyzing lesion area.

Statistical Analysis. The data were analyzed using a Mann–Whitney U test to compare two groups. When the data were normally distributed, Student t tests were performed. A P value <0.05 was considered statistically significant and represented with asterisks: $*P < 0.05$, $**P < 0.01$, $***P < 0.001$.

1. Gerlis LM (1956) The significance of adventitial infiltrations in coronary atherosclerosis. *Br Heart J* 18(2):166–172.
2. Jonasson L, Holm J, Skalli O, Bondjers G, Hansson GK (1986) Regional accumulations of T cells, macrophages, and smooth muscle cells in the human atherosclerotic plaque. *Arteriosclerosis* 6(2):131–138.
3. Hansson GK, Hermansson A (2011) The immune system in atherosclerosis. *Nat Immunol* 12(3):204–212.
4. Sohma Y, et al. (1995) Accumulation of plasma cells in atherosclerotic lesions of Watanabe heritable hyperlipidemic rabbits. *Proc Natl Acad Sci USA* 92(11):4937–4941.
5. Galkina E, et al. (2006) Lymphocyte recruitment into the aortic wall before and during development of atherosclerosis is partially L-selectin dependent. *J Exp Med* 203(5):1273–1282.
6. Lewis MJ, et al. (2009) Immunoglobulin M is required for protection against atherosclerosis in low-density lipoprotein receptor-deficient mice. *Circulation* 120(5):417–426.
7. Houtkamp MA, de Boer OJ, van der Loos CM, van der Wal AC, Becker AE (2001) Adventitial infiltrates associated with advanced atherosclerotic plaques: Structural organization suggests generation of local humoral immune responses. *J Pathol* 193(2):263–269.
8. Zhou X, Hansson GK (1999) Detection of B cells and proinflammatory cytokines in atherosclerotic plaques of hypercholesterolaemic apolipoprotein E knockout mice. *Scand J Immunol* 50(1):25–30.
9. Ylä-Herttuala S, et al. (1994) Rabbit and human atherosclerotic lesions contain IgG that recognizes epitopes of oxidized LDL. *Arterioscler Thromb* 14(1):32–40.
10. Caligiuri G, Nicoletti A, Poirier B, Hansson GK (2002) Protective immunity against atherosclerosis carried by B cells of hypercholesterolemic mice. *J Clin Invest* 109(6):745–753.
11. Kyaw T, et al. (2011) B1a B lymphocytes are atheroprotective by secreting natural IgM that increases IgM deposits and reduces necrotic cores in atherosclerotic lesions. *Circ Res* 109(8):830–840.
12. Major AS, Fazio S, Linton MF (2002) B-lymphocyte deficiency increases atherosclerosis in LDL receptor-null mice. *Arterioscler Thromb Vasc Biol* 22(11):1892–1898.
13. Kyaw T, et al. (2010) Conventional B2 B cell depletion ameliorates whereas its adoptive transfer aggravates atherosclerosis. *J Immunol* 185(7):4410–4419.
14. Ait-Oufella H, et al. (2010) B cell depletion reduces the development of atherosclerosis in mice. *J Exp Med* 207(8):1579–1587.
15. Hansson GK (2005) Inflammation, atherosclerosis, and coronary artery disease. *N Engl J Med* 352(16):1685–1695.
16. Chou MY, et al. (2009) Oxidation-specific epitopes are dominant targets of innate natural antibodies in mice and humans. *J Clin Invest* 119(5):1335–1349.
17. Duewell P, et al. (2010) NLRP3 inflammasomes are required for atherogenesis and activated by cholesterol crystals. *Nature* 464(7293):1357–1361.
18. Freigang S, et al. (2011) Nrf2 is essential for cholesterol crystal-induced inflammasome activation and exacerbation of atherosclerosis. *Eur J Immunol* 41(7):2040–2051.
19. Rajamäki K, et al. (2010) Cholesterol crystals activate the NLRP3 inflammasome in human macrophages: A novel link between cholesterol metabolism and inflammation. *PLoS ONE* 5(7):e11765.
20. Chen GY, Nuñez G (2010) Sterile inflammation: Sensing and reacting to damage. *Nat Rev Immunol* 10(12):826–837.
21. Gearhart PJ, Johnson ND, Douglas R, Hood L (1981) IgG antibodies to phosphorylcholine exhibit more diversity than their IgM counterparts. *Nature* 291(5810):29–34.
22. Shaw PX, et al. (2000) Natural antibodies with the T15 idiotype may act in atherosclerosis, apoptotic clearance, and protective immunity. *J Clin Invest* 105(12):1731–1740.
23. Palinski W, Miller E, Witztum JL (1995) Immunization of low density lipoprotein (LDL) receptor-deficient rabbits with homologous malondialdehyde-modified LDL reduces atherogenesis. *Proc Natl Acad Sci USA* 92(3):821–825.
24. Caligiuri G, et al. (2007) Phosphorylcholine-targeting immunization reduces atherosclerosis. *J Am Coll Cardiol* 50(6):540–546.
25. Binder CJ, et al. (2003) Pneumococcal vaccination decreases atherosclerotic lesion formation: Molecular mimicry between Streptococcus pneumoniae and oxidized LDL. *Nat Med* 9(6):736–743.
26. Binder CJ, et al. (2004) IL-5 links adaptive and natural immunity specific for epitopes of oxidized LDL and protects from atherosclerosis. *J Clin Invest* 114(3):427–437.
27. Binder CJ, et al. (2005) The role of natural antibodies in atherogenesis. *J Lipid Res* 46(7):1353–1363.
28. Faria-Neto JR, et al. (2006) Passive immunization with monoclonal IgM antibodies against phosphorylcholine reduces accelerated vein graft atherosclerosis in apolipoprotein E-null mice. *Atherosclerosis* 189(1):83–90.
29. Choi YS, Dieter JA, Rothaeusler K, Luo Z, Baumgarth N (2012) B-1 cells in the bone marrow are a significant source of natural IgM. *Eur J Immunol* 42(1):120–129.
30. Shaw PX, Goodyear CS, Chang MK, Witztum JL, Silverman GJ (2003) The autoreactivity of anti-phosphorylcholine antibodies for atherosclerosis-associated neo-antigens and apoptotic cells. *J Immunol* 170(12):6151–6157.
31. Martin F, Oliver AM, Kearney JF (2001) Marginal zone and B1 B cells unite in the early response against T-independent blood-borne particulate antigens. *Immunity* 14(5):617–629.
32. Kraal G, Mebius R (2006) New insights into the cell biology of the marginal zone of the spleen. *Int Rev Cytol* 250:175–215.
33. Wardemann H, Boehm T, Dear N, Carsetti R (2002) B-1a B cells that link the innate and adaptive immune responses are lacking in the absence of the spleen. *J Exp Med* 195(6):771–780.
34. Wermeling F, et al. (2007) Class A scavenger receptors regulate tolerance against apoptotic cells, and autoantibodies against these receptors are predictive of systemic lupus. *J Exp Med* 204(10):2259–2265.
35. Chang MK, et al. (2004) Apoptotic cells with oxidation-specific epitopes are immunogenic and proinflammatory. *J Exp Med* 200(11):1359–1370.
36. Ma Z, et al. (2008) Accelerated atherosclerosis in ApoE deficient lupus mouse models. *Clin Immunol* 127(2):168–175.
37. Johnson SA, Rozzo SJ, Cambier JC (2002) Aging-dependent exclusion of antigen-inexperienced cells from the peripheral B cell repertoire. *J Immunol* 168(10):5014–5023.
38. Maseda D, et al. (2012) Regulatory B10 cells differentiate into antibody-secreting cells after transient IL-10 production in vivo. *J Immunol* 188(3):1036–1048.
39. Vale AM, et al. (2013) The link between antibodies to OxLDL and natural protection against pneumococci depends on D(H) gene conservation. *J Exp Med* 210(5):875–890.
40. Lötscher M, Amstutz H, Heusser CH, Blaser K (1990) Fine specificity and heavy chain V gene usage of antibodies to the phosphorylcholine hapten. *Mol Immunol* 27(4):369–378.

41. Jordö ED, Wermeling F, Chen Y, Karlsson MC (2011) Scavenger receptors as regulators of natural antibody responses and B cell activation in autoimmunity. *Mol Immunol* 48(11):1307–1318.

42. Yvan-Charvet L, et al. (2007) Combined deficiency of ABCA1 and ABCG1 promotes foam cell accumulation and accelerates atherosclerosis in mice. *J Clin Invest* 117(12): 3900–3908.

43. Binder CJ, Silverman GJ (2005) Natural antibodies and the autoimmunity of atherosclerosis. *Springer Semin Immunopathol* 26(4):385–404.

44. Masmoudi H, Mota-Santos T, Huetz F, Coutinho A, Cazenave PA (1990) All T15 Id-positive antibodies (but not the majority of VHT15+ antibodies) are produced by peritoneal CD5+ B lymphocytes. *Int Immunol* 2(6):515–520.

45. Hamaguchi Y, et al. (2005) The peritoneal cavity provides a protective niche for B1 and conventional B lymphocytes during anti-CD20 immunotherapy in mice. *J Immunol* 174(7): 4389–4399.

46. Yu S, Dunn R, Kehry MR, Braley-Mullen H (2008) B cell depletion inhibits spontaneous autoimmune thyroiditis in NOD.H-2h4 mice. *J Immunol* 180(11):7706–7713.

47. Robinette CD, Fraumeni JF, Jr (1977) Splenectomy and subsequent mortality in veterans of the 1939-45 war. *Lancet* 2(8029):127–129.

48. Aviram M, Brook JG, Tatarsky I, Levy Y, Carter A (1986) Increased low-density lipoprotein levels after splenectomy: A role for the spleen in cholesterol metabolism in myeloproliferative disorders. *Am J Med Sci* 291(1):25–28.

49. Havel RJ, Eder HA, Bragdon JH (1955) The distribution and chemical composition of ultracentrifugally separated lipoproteins in human serum. *J Clin Invest* 34(9):1345–1353.

50. Puhl H, Waeg G, Esterbauer H (1994) Methods to determine oxidation of low-density lipoproteins. *Methods Enzymol* 233:425–441.

51. Zhang L, et al. (2012) The tryptophan metabolite 3-hydroxyanthranilic acid lowers plasma lipids and decreases atherosclerosis in hypercholesterolaemic mice. *Eur Heart J* 33(16):2025–2034.

52. Mevorach D, Zhou JL, Song X, Elkon KB (1998) Systemic exposure to irradiated apoptotic cells induces autoantibody production. *J Exp Med* 188(2):387–392.

53. Matsushita T, Tedder TF (2011) Identifying regulatory B cells (B10 cells) that produce IL-10 in mice. *Methods Mol Biol* 677:99–111.

54. Walter JE, et al. (2010) Expansion of immunoglobulin-secreting cells and defects in B cell tolerance in Rag-dependent immunodeficiency. *J Exp Med* 207(7):1541–1554.

55. Nicoletti A, Kaveri S, Caligiuri G, Bariéty J, Hansson GK (1998) Immunoglobulin treatment reduces atherosclerosis in apo E knockout mice. *J Clin Invest* 102(5): 910–918.